

## CO-Simulation Analysis of Hydraulic Steel-Belt Overwind Buffer Device

Wu Juan and Kou Ziming

College of Mechanical Engineering, Taiyuan University of  
Technology, Taiyuan 030024, China

**Abstract:** In this study, we obtain overwind buffer distance by using the Lagrange equation to establish the two-degrees-of-freedom mathematical model with vertical shaft lifting system in rolling process. Design of a buffer device which is composed of a hydraulic energy absorption and strip plastic deformation energy absorbing and analyze its working principle with mechanical and hydraulic system. Analysis of the overwind buffer time and buffer distance with loaded full overwind and no-load speed by using ADAMS and AMESim to build mechanical hydraulic combined simulation model of hydraulic steel-belt overwind buffer device. The simulation results show that: buffer time is 0.67 sec and buffer distance is 0.38 m with loaded full overwind; buffer time is 0.523 sec and buffer distance is 0.05 m with no-load speed overwind. The design of Hydraulic steel-belt overwind buffer device conforms with the requirements of safety regulation in coal mine.

**Keywords:** Buffer, hydraulic energy absorption, mechanical-hydraulic coupling simulation

### INTRODUCTION

With the extensive use of vertical shaft hoisting system in the mine hoist system, the vertical shaft hoisting system has become the key to the efficient and safe production of the mine (Jiang, 2008). Although the vertical shaft hoisting system has a variety of electrical protection and backup protection, overwind accidents still happen frequently due to high container speed and certain restrictions in braking deceleration when overwind. At present there are wedge-shaped cans road, buffered wood (bumper beam), friction energy absorbing devices in overwind buffer mining equipments of national mine (Xi-Ping, 2009; Jia-Feng, 2010). Literature 3-7 (Guo-Wang and Chun-Xiao, 2007; Li, 2009) analyses several overwind buffer devices. Literature 8 (Jin-Hua *et al.*, 2010) has a stress analysis of vertical shaft hoisting anti-overwind and anti-overdischarge buffer supporting cage devices. Literature 9 (Fu-Zhen *et al.*, 2011; Yu-Jin, 2008) adopts COSMOS Motion to have a simulation analysis of hoisting over rolling buffering devices. Along with the introduction of steel-belt type plastic deformation absorption, plastic deformation absorption overwind buffer device has widely applied in various mines. Based on plastic deformation absorption overwind buffer device, this study studies a hydraulic steel-belt overwind buffer device and conducts a mechanical-hydraulic liquid joint simulation test for the buffer process of the device (Yong-Zhou and Ji-Sheng, 2009; Yang-Rui *et al.*, 2012).

### METHODOLOGY

**Dynamic analysis of buffer process of vertical shaft hoisting system:** The quality of the down side of the cage can be ignored. Using Lagrange equation to establish 2-d mathematical model of friction type upgrade system over rolling process, as is shown in Fig. 1. Lagrange equation is:

$$\frac{d}{dt} \left( \frac{\partial T}{\partial \dot{q}_i} \right) - \frac{\partial T}{\partial q_i} + \frac{\partial U}{\partial q_i} = Q_i \quad (1)$$

where,

- T = The kinetic energy of the lifting system
- U = The potential energy of the lifting system
- Q<sub>i</sub> = The generalized force of the lifting system
- q<sub>i</sub> = The generalized of the lifting system

The kinetic energy of the system is:

$$T = \frac{1}{2} m_2 \dot{x}_2^2 + \frac{1}{2} m_3 \dot{x}_3^2 + \frac{1}{6} m_x \dot{x}_3^2 + \frac{1}{3} m_t \frac{\dot{x}_2^2 + \dot{x}_2 \dot{x}_3 + \dot{x}_3^2}{2} \quad (2)$$

The potential energy of the system is:

$$U = -m_x g x_3 + m_2 g x_2 + \frac{1}{2} m_t g (x_2 + x_3) + k x_2^2 + \frac{1}{2} k_2 (x_3 - x_2 + f_s)^2 \quad (3)$$

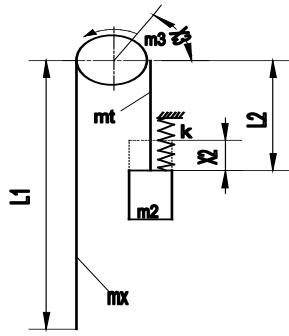


Fig. 1: Overwind buffer process mathematical model with two degrees of freedom

where,

$k$  = The elasticity coefficient of the buffer device, N/m

$k_2$  = The elasticity coefficient of the rising side of the rope  $k_2 = \frac{EA}{L_2}$ , N/m

$A$  = The elasticity modulus of the rope, mm<sup>2</sup>

$L_2$  = The length of the rising side of the rope, m

$f_2$  = The initial displacement of the rising side of the rope

$$f_s = \frac{m_2 g}{k_2} + \frac{m_t g}{2k_2}, m$$

The generalized force  $Q_2 = 0$

The generalized force  $Q_3 = (m_2 + m_t - m_x) g$

According to Lagrange Eq. (2) freedom differential equation of the system is:

$$\begin{cases} (m_2 + \frac{m_t}{3})\ddot{x}_2 + \frac{1}{6}m_t\ddot{x}_3 + (2k - k_2)x_2 + k_2x_3 = 0 \\ (m_3 + \frac{m_x + m_t}{3})\ddot{x}_3 + \frac{1}{6}m_t\ddot{x}_2 - k_2x_2 + k_2x_3 = 0 \end{cases} \quad (4)$$

The initial condition is:

$$\{x_0\} = \{0\}, \{\dot{x}_0\} = \{V\}$$

Write type (4) as universal differential equations of two freedom degree of the system:

$$\begin{cases} a_{11}\ddot{x}_2 + a_{12}\ddot{x}_3 + c_{11}x_2 + c_{12}x_3 = 0 \\ a_{21}\ddot{x}_2 + a_{22}\ddot{x}_3 + c_{21}x_2 + c_{22}x_3 = 0 \end{cases} \quad (5)$$

where,

$$a_{11} = m_2 + (m_t/3)$$

$$a_{12} = a_{21} = (1/6 m_t)$$

$$a_{22} = m_3 + ((m_x + m_t) / 3)$$

$$\begin{aligned} c_{11} &= 2k - k_2 \\ c_{12} &= c_{22} = k_2 \\ c_{21} &= -k_2 \\ x_2 &= A_1 \sin(Pt + \alpha_1) \\ x_3 &= A_2 \sin(Pt + \alpha_2) \end{aligned}$$

substitution type (5):

$$\begin{cases} -A_1 p^2 a_{11} - A_2 P^2 a_{12} + c_{11} A_1 + c_{12} A_2 = 0 \\ -A_1 P^2 a_{21} - A_2 P^2 a_{22} + c_{21} A_1 + c_{22} A_2 = 0 \end{cases} \quad (6)$$

Type (6) can be obtained, respectively:

$$\frac{A_1}{A_2} = -\frac{c_{12} - a_{12}P^2}{c_{11} - a_{11}P^2}, \frac{A_1}{A_2} = -\frac{c_{22} - a_{22}P^2}{c_{21} - a_{12}P^2}$$

By finishing:

$$(c_{11} - a_{11}P^2)(c_{22} - a_{22}P^2) - (c_{21} - a_{12}P^2)^2 = 0 \quad (7)$$

So the vibration frequency of this system is:

$$\begin{cases} P_1^2 = \frac{-B - \sqrt{B^2 - 4AC}}{2A} \\ P_2^2 = \frac{-B + \sqrt{B^2 - 4AC}}{2A} \end{cases} \quad (8)$$

where,

$$A = a_{11}a_{22} - a_{12}^2$$

$$B = 2a_{12}c_{12} - a_{11}c_{22} - a_{22}c_{11}$$

$$C = c_{11}a_{22} - c_{12}^2$$

The general solution of the equation:

$$\begin{cases} x_2 = A_{11} \sin(P_1 t + \alpha_1) + A_{12} \sin(P_2 t + \alpha_2) \\ x_3 = A_{21} \sin(P_1 t + \alpha_1) + A_{22} \sin(P_2 t + \alpha_2) \end{cases} \quad (9)$$

### The design of hydraulic steel-belt overwind buffer device:

**The mechanical design:** As is shown in Fig. 2, hydraulic steel-belt overwind buffer device can be divided into three parts: Overwind buffer part, holding tank portion and volume restoration part.

Overwind buffer portion is composed of a hydraulic buffer mechanism and the tape buffer mechanism. Hydraulic buffer mechanism is composed of cushion cylinder, beams and the corresponding hydraulic components; strip buffer mechanism is composed of steel, column, a sliding column, the support plate and the pressure roller and so on. When overwind occurs, ascending vessel push beam upward and beam through the connection with the shaft pin takes with buffer oil cylinder piston rod and smooth

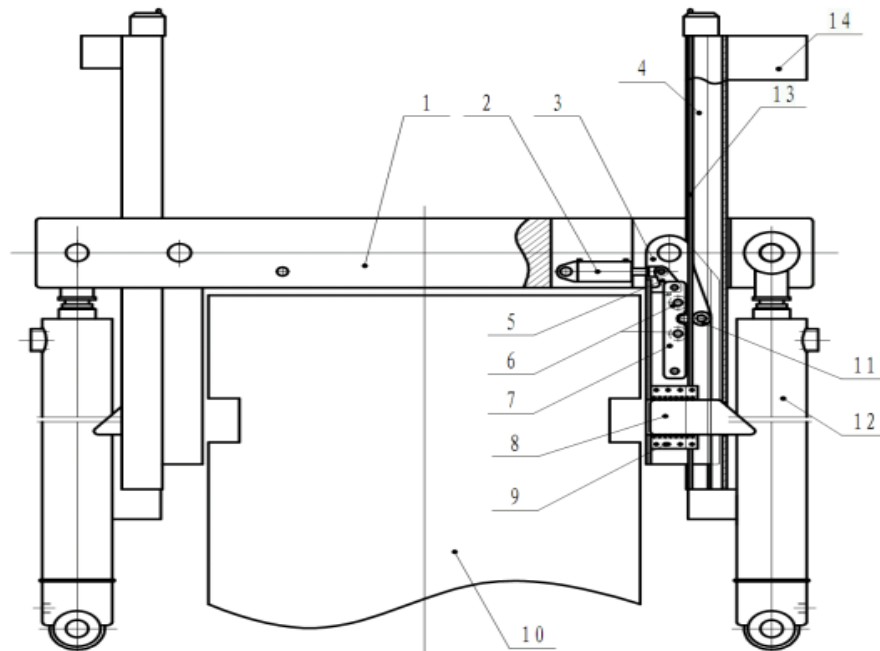


Fig. 2: Hydraulic steel-belt overwind buffer

- 1: Beam; 2: Buffer oil cylinder; 3: Slippy column; 4: Pillar; 5: Fork; 6: Press roller; 7: Support plate; 8: The lock tongue; 9: The lock tongue tracks; 10: Lifting container; 11: Middle pressure roller; 12: Buffer oil cylinder; 13: Steel belt; 14: Mast

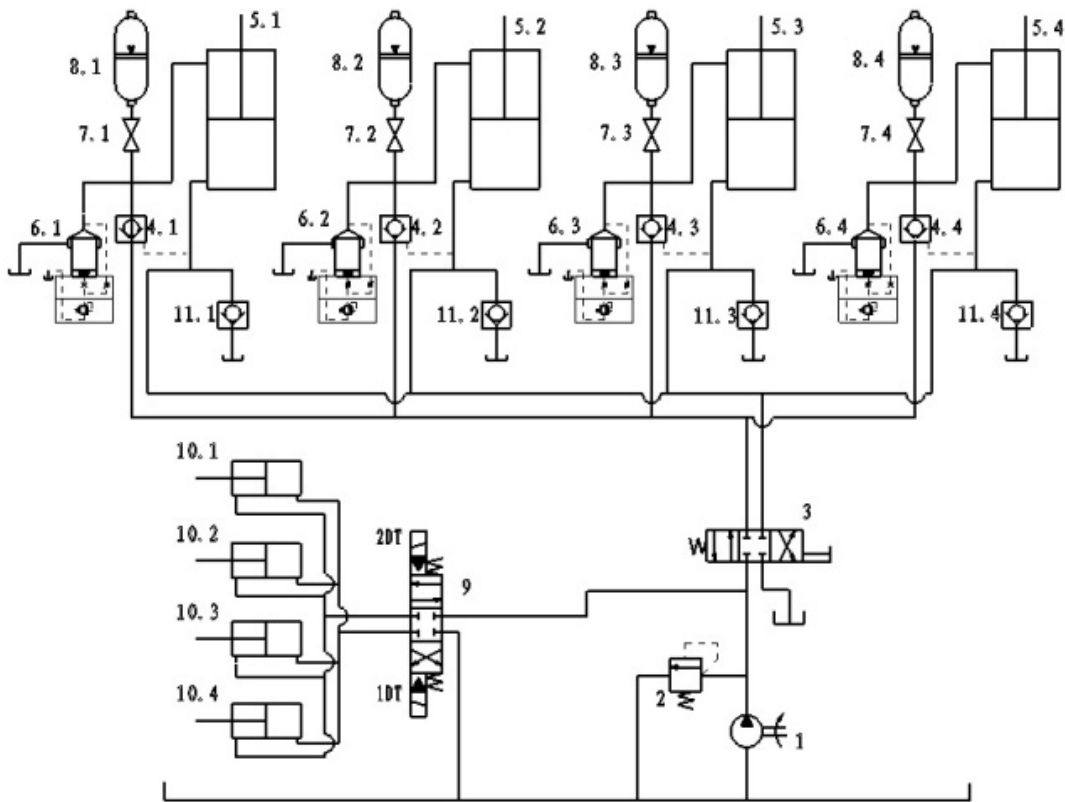


Fig. 3: The hydraulic schematic diagram

- 1: Pump; 2: Relief valve; 3: Reversing valve; 4: Liquid control one-way valve; 5: Buffer oil cylinder; 6: Cartridge relief valve; 7: Cut-off valve; 8: Accumulator; 9: Electromagnetic reversing valve; 10: Recovery cylinder

column together to move up; when the hydraulic system pressure reaches the set point, it begins to overflow absorption; a sliding column takes with top and bottom pressure roller and intermediate pressure roller to move, intermediate pressure roller conduct horizontal motion to hoisting container lateral with the oppression of the pillar crankshaft. Thus it makes steel belt with the press from top and bottom pressure roller and intermediate pressure roller occur the deformation of S type so as to absorb energy. Under the common function of hydraulic absorption and plastic deformation absorption, ascending vessel finally stops smoothly.

Holding tank portion is composed of the lock tongue, a lock tongue cage guide rail and the sliding column. In the buffer process lock tongue with sliding column rising in column, in the column the force next level stretched out and into the upper footwall ascending vessel, so that ascending vessel will move along with slide column, beams whether it moves up or down.

An overwind recovery portion is composed of the restoration of oil cylinder, fork, the support plate and the sliding column. When the end of overwind needed to restore, recover oil cylinder piston rod extends out so as to make fork winding rotate around pin shaft which is connected to the supporting plate and to drive the support plate to incline in the ascending vessel side and the distance between top and bottom pressure roller and intermediate pressure roller of the support plate increases, which makes steel belt move freely. The

buffer oil cylinder piston rod is retracted and ultimately the lifting container move back into its normal position.

Figure 2 the structure of the utility model has the advantages of hydraulic energy absorption and the plastic deformation energy absorbing work together so as to effectively improve the reliability of overwind buffer. The lock tongue can effectively hold back the back ascending vessel and the quality load of the ascending vessel is taken by buffer oil cylinder and steel belt that improves the safety. Recovery part composed of recovery oil cylinder and support plate and other components can make overwind recovery process safely, simply and quickly finish.

**Design of hydraulic system:** The hydraulic system (Fig. 3) of hydraulic steel-belt overwind buffer device is composed of the overwind buffer loop, overwind recovery loop and control loop. The overwind buffer loop is the core loop of hydraulic system which is mainly composed of a one-way valve-11, a buffer oil cylinder-5, cartridge relief valve-6 and a fuel tank. Overwind recovery loop is mainly composed of an oil pump-1, an electromagnetic reversing valve-9, recovery cylinder-10 and a fuel tank, which is the essential part that promised volume restoration process safety and fast realization. Control loop is mainly composed of an oil pump-1, a reversing valve-3, a liquid control one-way valve-4, a buffer cylinder-5 and a fuel tank, which plays an important role in equipment installation and debugging process.

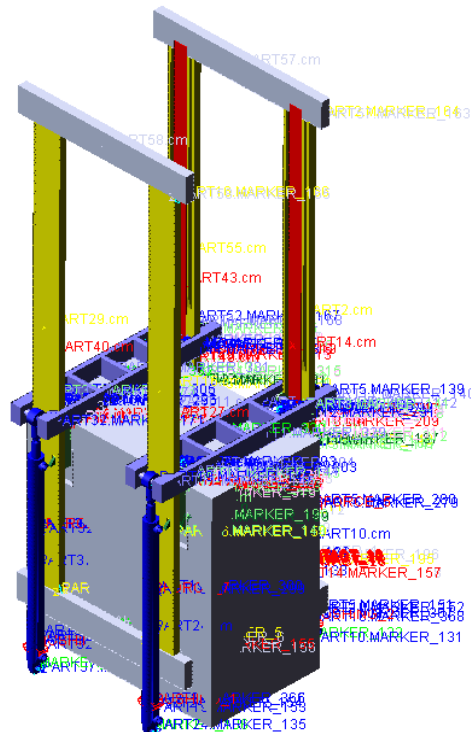


Fig. 4: The simulation model in ADAMS

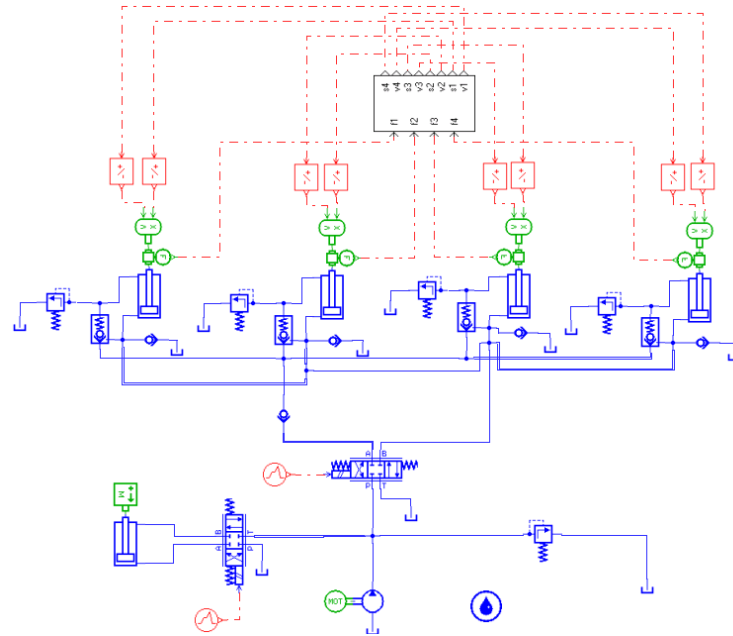


Fig. 5: Machine hydraulic coupling simulation model

Hydraulic steel-belt overwind buffer device use a energy absorbing mode that hydraulic energy absorber and steel plastic deformation energy absorbing synergy absorption to absorb hoisting container overwind impact energy. Hydraulic energy absorbing can play a leading role and steel belt plastic deformation energy absorbing as an auxiliary function in the wind buffer process. It can effectively enhance the overwind buffer device cushioning performance and ensure safely and stably lifting container dock. The steel belt can be repeatedly used, because the steel belt deformation as an auxiliary function, the deformation is small and the force is smaller, so the steel belt bears little damage in the buffer process.

#### Research on simulation:

**Machine-fluid co-simulation modeling:** A virtual prototype model of the hydraulic strip of overwind buffer device be built in Dynamic simulation software ADAMS (Xiao-Ming and Zhao-Mei, 2011), shown in Fig. 4. Hydraulic system simulation model be built in AMESim software environment. After the two models are built, interface module of machine-fluid coupling simulation be outputted in ADAMS and be imported the hydraulic model in AMESim environment (Zhu *et al.*, 2011a), shown in Fig. 5.

### MACHANICAL AND HYDRAULIC JOINT SIMULATION TEST AND RESULTS ANALYSIS

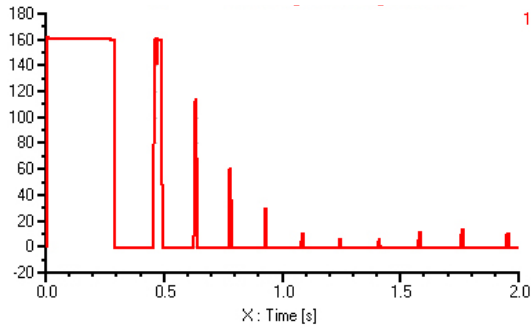
A hypothesis of hoisting system happened respectively overwind status in full load speed and

Idling speed conditions, loaded with full speed when overwind hoisting container quality 12 tons, the rising speed of 10 m/sec; relief valve pressure setting for 16 MPa. No load with low speed when overwind hoisting container quality 6 tons, the rising speed of 3 m/sec; relief valve pressure setting for 16 MPa. Oil cylinder stem diameter and cylinder size are 60 and 90 mm; deformation resistance of steel belt is applied between the steel belt and the sliding column of virtual prototype in ADAMS environment (apply force to replace deformation resistance of steel strip). Through operating simulation model in the AMESim software, finally we get the simulation curve as shown in the Fig. 6a, b, c, d and 7a, b, c, d.

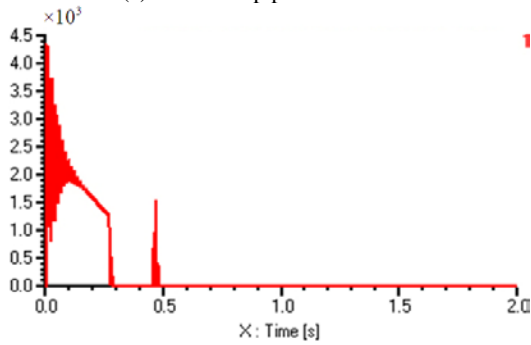
**The full-load overwind with full speed:** As is shown in Fig. 6a, about at 0.67 sec in the overwind buffer process, buffer loop pressure is lower than 10 MPa. At 0.67 sec buffer loop does not appear the overflow condition in the Fig. 6b. So is thought that buffer time is about 0.67 sec. Meeting the theory to calculate the required buffer time is 0.5-1 sec requirements.

Hoisting container in the rise to the highest point will appear the fall situation back (Fig. 6c). From the curves, hoisting container maximum upward position is 2.95 M and the lowest downward position is 2.57 M, so buffer distance of hoisting container is 0.38 m. Meet the "coal mine safety regulation" (Zhu *et al.*, 2011b) regulation of buffer distance less than or equal to 0.5 m and maximum overwind distance requirements.

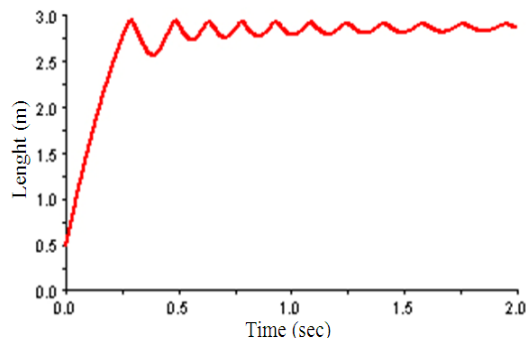
From Fig. 6d, It is known that hoisting container (hoisting container just contact beams) appeared



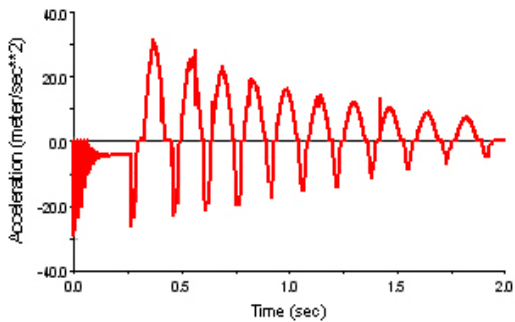
(a) Buffer loop pressure curve



(b) Buffer loop flow curve



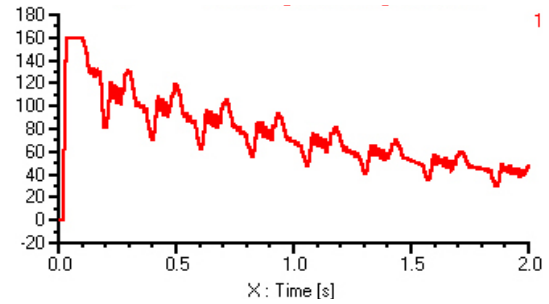
(c) The displacement curve of hoisting container



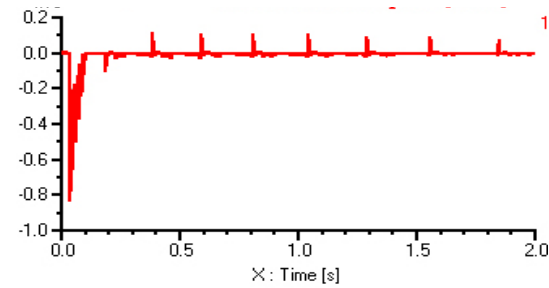
(d) The acceleration curve of hoisting container

Fig. 6: The full-loading buffer loop curve when over wind

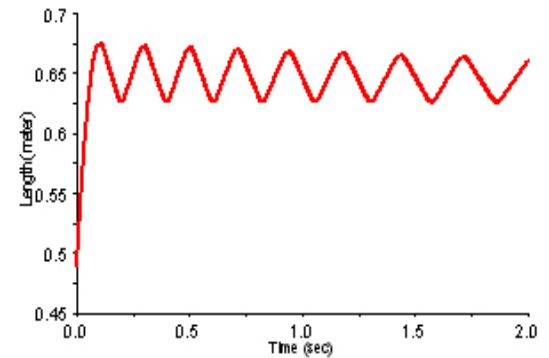
intense fluctuations with acceleration in the initial stage of buffer, then acceleration tends smooth; acceleration



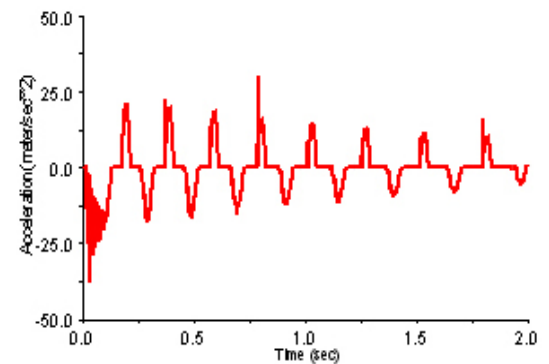
(a) Buffer loop pressure curve



(b) Buffer loop flow curve



(c) The displacement curve of hoisting container



(d) The acceleration curve of hoisting container

Fig. 7: The curve of no-loading buffer oil cylinder when over wind

appears bigger wave motion in about 0.25 sec, that is because hoisting container reach the highest point then

drop back. From the curves, in the buffer process the maximum acceleration is about  $28.78 \text{ m/sec}^2$ . Meet the buffer acceleration is about 1-3 times gravity acceleration requirements.

**The no-load overwind with a low speed:** Figure 7a shows, at 0.523 sec buffer loop pressure is lower than 10 Mpa. From the Fig. 7b, it is known that in 5.23 sec overflow are not present in the buffer loop, so the buffer time is 0.523 sec, which meets the design requirements.

As shown in Fig. 7c, the highest position of hoisting container is 0.68 m, the lowest position is 0.63 M, so the buffer distance is 0.05 m, which meets the requirements of buffer distance: buffer distance not greater than 0.5 m.

In Fig. 7d, hoisting container maximum buffer acceleration is  $37.03 \text{ m/sec}^2$ . The acceleration appeared to fluctuate from 0s to 0.12 sec, about after 0.13 sec acceleration appeared periodic reductive gradually changes. Although the biggest buffer acceleration of  $37.03 \text{ m/sec}^2$  is not in the range of (1-3) g, but  $37.03 \text{ m/sec}^2$  only appears at 0.003 sec, the others all meet buffer acceleration is about (1-3) g requirements. It is suggested that the simulation results meet the design requirements.

By full-load full speed and no-load low speed overwind simulation result analysis, the design of the hydraulic steel-belt overwind buffer device either in full-load full speed or in no-load low speed overwind in the buffer time, buffer distance, the buffer acceleration and other technical requirements all meet the design requirements.

## CONCLUSION

- By Lagrange equation it is to establish the two degree freedom mathematical model of friction upgrade the overwind process in order to analyze the volume of buffer distance.
- Design a overwind buffer device of hydraulic steel belt. The hydraulic absorption and steel belt plastic deformation absorption can be a combination of energy absorption model, which can effectively enhance the overwind buffer performance. The absorption model of hydraulic absorption as the main role and steel belt plastic deformation energy absorption as the supplementary role, can achieve the reuse of the overwind buffer device.
- Through the machine-fluid coupling simulation results shows that: full load at full speed through overwind, buffer time is 0.67 sec and distance is 0.38 m. No-load low-speed over the overwind, buffer time is 0.523 sec and distance is 0.05 m. These parameters meet the regulations requirement.

## ACKNOWLEDGMENT

The authors wish to thank the helpful comments and suggestions from my teachers and colleagues. This study is supported by National Natural Science Fund (No. 51205272) and National Science and Technology Cooperation Fund (2011DFA72120).

## REFERENCES

- Fu-Zhen, Y., B. Xiao and C. Zhe, 2011. Force Analysis about over wind and over relaxation precaution of buffering and supporting cage device in vertical mine. *Coal Mine Mach.*, 32(7): 70-71.
- Guo-Wang, Z. and L. Chun-Xiao, 2007. Comparison of equipments for impact-resistance, cushioning in reeling and bracketing cage protection between two vertical elevating systems. *Coal Mine Mach.*, 28(8): 134-136.
- Jia-Feng, W., 2010. Application of over wind buffer and supporting anti-tank devices and squat cage device. *Coal Technol.*, 29(4).
- Jiang, X.H., 2008. Study on the safety and reliability of vertical hoisting shaft system [D]. MA Thesis, China University of Mining and Technology, XuZhou, China.
- Jin-Hua, P., Z. Hong-Xiao and L. Yuan-Sheng, 2010. The application of HZSN type hoist multi-function over winding protection device in chaohua coal mine. *Zhongzhou Coal*, (1): 59-60.
- Li, Y.J., 2009. Actuality and direction of over wind buffers in mining hoist. *Min. Process. Equipment*, 37(13): 57-61.
- Xi-Ping, W., 2009. Several types of over wind buffer and supporting cage device. *Coal Mine Mach.*, 30(3): 122-124.
- Xiao-Ming, Z. and X. Zhao-Mei, 2011. Winder based COSMOS motion over wind buffer device simulation analysis. *Coal Mine Mach.*, 31(2): 86-88.
- Yang-Rui, C., K. Zi-ming and L. Zhi, 2012. Hydraulic over rolling buffering devices of theory analysis. *Coal Mine Mach.*, 33(5): 93-95.
- Yong-Zhou, Z., A. Ji-Sheng and L. Yang, 2009. The HZSN overreach protector used in mine lifting system. *Min. Process. Equipment*, 32(13): 105-106.
- Yu-Jin, L., 2008. Multirope Friction to Enhance the System Dynamics and Engineering Design [M]. China Coal Industry Publishing House, China, Vol. 12.
- Zhu, X., L. Quan, X. Wang, X. Lü and G. Li, 2011a. Co-simulation analysis of working characteristic for large hydraulic excavator. *J. Agric. Mach.*, 42(4): 27-32.
- Zhu, X., L. Quan, X. Wang, X. Lü and G. Li, 2011b. Co-simulation of flat-pushing characteristics of large mining face-shovel hydraulic excavator. *J. Agric. Mach.*, 42(5): 30-34.